

# Verification of the Optimum Predicting Model for Dye-Based Inkjet Printer

Takayuki Ogasahara and Noboru Ohta

CANON INC. and Munsell Color Science Laboratory, Rochester Institute of Technology  
Rochester, New York

## Abstract

It is very important to fully understand the relationship between ink placed on paper and the resultant colorimetry for image quality improvement. Success will enable one to develop a simulation that can be used to design optimum subtractive color dyes for any criterion. The purpose of the present study is to establish a systematic understanding of color reproduction systems of the present-day subtractive color inkjet printer (IJ). In general, dyes used in formulating inks for current IJs have color gamuts larger than those obtained by pigments. The dye technology is advancing rapidly, and tools are needed to select an optimal dye set from among many potential dyes. In the present study, the predicting models such as the Neugebauer model, the Yule-Nielsen Neugebauer model, the Kubelka-Munk model, the Cellular Neugebauer model, and the Cellular Kubelka-Munk model built for use in photography and traditional printing systems have been verified for dye-based IJ. Furthermore the comparison between IJ and photography has been studied by means of a computer simulation method. The study has been carried out from the viewpoints of the stability of selective grays for illumination metamerism and of maximizing color gamut volumes. This study is an important step toward the development of simulations for use in improving image quality for the present-day subtractive color IJ.

## Introduction

Recently IJs have been rapidly advancing. Among a variety of factors controlling image quality of IJs, granularity and tone reproduction have been improved considerably by ink dilution and small droplet technology. For further improvement of image quality, it is very important to realize increasing the size of the color gamut of subtractive color dyes. Development for the optimum subtractive color dyes needs to fully understand the relationship between ink placed on paper and the resultant colorimetry. In the field of photography and printing, the models used to predict reproduced tristimulus values from dye amounts, including the Neugebauer model, the Yule-Nielsen Neugebauer model, and the Kubelka-Munk model.<sup>1-4</sup>

Recently IJs have a tendency to use dyes in order to realize larger color gamuts. However, there are few studies

for dye-based IJs, so establishment of the optimum predicting model is necessary. The present study has compared five predicting models for dye-based IJs. Further, optimum subtractive color dyes in a color film and a color paper have previously been studied by means of computer simulation for maximum stability of gray balance and color gamut.<sup>5-7</sup> In follow-up to those studies, two factors are compared here for controlling image quality between dye-based IJ and color photography (a color print) by using the optimum predicting model and computer simulation.

## Predicting Models

The Neugebauer model (NM)<sup>8</sup> has been widely used for modeling binary color printers. It is the multi-colorant generalization of Murray-Davies equation<sup>9</sup> that predicts the reflectance of multi-colorant mixtures in halftone printing. The Neugebauer equation is written as follows:

$$\hat{R}_\lambda(\lambda) = \sum_i p_i R_{\lambda,i}(\lambda) \quad (1)$$

where  $\hat{R}_\lambda(\lambda)$  is the predicted spectral reflectance,  $R_{\lambda,i}(\lambda)$  represents the measured spectral reflectance of Neugebauer primaries, and  $p_i$  is the weight applied to the  $i^{\text{th}}$  Neugebauer primary. If the dot locations for colorants are placed using a random or rotated screen,<sup>10,11</sup> Demichel equation<sup>12</sup> is assumed to hold, the primary set is shown below for a set of  $i$  colorants:

$$\begin{aligned} p_1 &= (1 - a_{\text{colorant1}})(1 - a_{\text{colorant2}}) \cdots \\ p_2 &= a_{\text{colorant1}}(1 - a_{\text{colorant2}}) \cdots \\ p_3 &= (1 - a_{\text{colorant1}})a_{\text{colorant2}} \cdots \\ &\vdots \\ p_i &= a_{\text{colorant1}} a_{\text{colorant2}} \cdots \end{aligned} \quad (2)$$

where  $a_{\text{coloranti}}$  is the area covered by  $i^{\text{th}}$  primary colorant. This area can often be calculated by using a regression.

However there is considerable difference between the reflectance predicted by NM and the measured reflectance because of the effect of light scattering in the paper. Therefore Yule-Nielsen<sup>13</sup> modified the Neugebauer

equation to predict results in the presence of light scattering. The Yule-Nielsen Neugebauer equation (YNNM) is written as follows:

$$\hat{R}_\lambda(\lambda) = \left( \sum_i p_i R_{\lambda,i,\max}^{1/n}(\lambda) \right)^n \quad (3)$$

where  $n$  is Yule-Nielsen factor. Typically  $n$  is determined through minimizing some metric such as  $\Delta E_{94}$  or Spectral Reflectance RMS error.

The Kubelka-Munk model (KMM),<sup>14</sup> which was developed as a series of equations useful for predicting reflectance in many types of colorant systems, is often used as an approach for translucent and opaque media. The Kubelka-Munk equation is written as follows:

$$\hat{R}_\lambda(\lambda) = R_{\lambda,paper}(\lambda) \exp \left\{ -2 \left( \sum_i c_i k_{\lambda,i} \right) \right\} \quad (4)$$

$$k_{\lambda,i} = -0.5 \ln \{ R_{\lambda,i}(\lambda) / R_{\lambda,paper}(\lambda) \} \quad (5)$$

where,  $R_{\lambda,paper}$  is the spectral reflectance of the paper,  $c$  represents concentration and  $k_\lambda$  defines the absorptivity of each colorant.

To better predict reflectance, the Cellular Neugebauer model (CNM)<sup>15,16</sup> restricts the effective area coverage used by the Neugebauer equation within narrow limits geometrically that is shown in Fig. 1 and written as follows:

$$a'_{eff} = \frac{a_{eff} - a_{eff,lower}}{a_{eff,upper} - a_{eff,lower}} \quad (6)$$

where,  $a'_{eff}$  is normalized effective area coverage based on the upper and lower bounding area coverage of the cell. The Cellular Kubelka-Munk model (CKMM)<sup>17</sup> restricts the concentration used by the Kubelka-Munk equation within narrow limits geometrically as same as CNM.

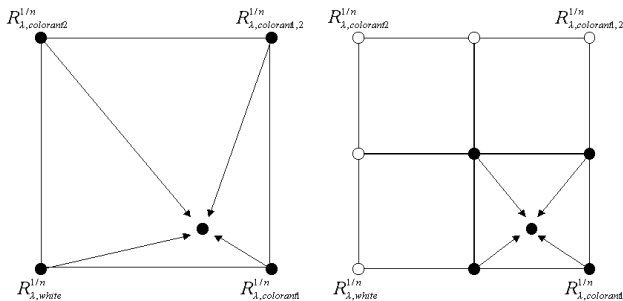


Figure 1. Illustration of two-colorant model. Left side is NM that has 4 primaries and the area coverage of 0% and 100%. Right side is CNM that has  $3^2 = 9$  primaries and the area coverage of 0%, 50%, and 100%. Solid circles show Neugebauer primaries.

### Experimental Results

A CANON S900 was used as a dye-based IJ. In fact, the IJ employs six inks by cyan (C), magenta (M), yellow (Y), black (K), 1/6 density photo cyan (PC), and 1/6 density

photo magenta (PM) and its printing resolution is 1200dpi×1200dpi. In this present study, four inks as CMYK and a coated paper (Professional Photo Paper) were used. A GretagMacbeth SpectroScan spectrophotometer was used to make all the spectral measurements. The predicting models described above were used and compared: NM, YNNM ( $n = 10.0$ ), KMM, CNM ( $n = 10.0$ ), and CKMM.

### Two-Colorant Model Evaluation

486 (81×6) printed samples that composed of two colorants as CM, CY, CK, MY, MK, and YK were used for evaluation of each predicting model. CNM and CKMM models used the effective area coverage and concentration of 0%, 50%, and 100% so the set of primaries was  $3^2 = 9$ . CNM and CKMM were better results than others by  $\Delta E_{94}$  and Spectral Reflectance RMS error.  $\Delta E_{94}$  was improved about twice from YNNM to CNM and about three times from KMM to CKMM in Table 1.

Table 1. Comparison of Prediction Accuracy Among Predicting Models.

	NM	YNNM	KMM	CNM	CKMM
$\Delta E_{94}$ D65	5.56	3.59	6.54	1.92	2.15
Std.	3.28	2.13	4.39	1.42	1.69
Maximum	14.92	10.20	20.47	8.40	8.98
Minimum	0.05	0.03	0.00	0.04	0.00
$\Delta E_{94}$ ill A	5.63	3.63	6.81	1.90	2.24
RMS	0.048	0.029	0.027	0.017	0.013

### Three-Colorant Model Evaluation

CNM and CKMM were focused from the result of two-colorant model evaluation. Product development requirements for a set of primaries are typically where prediction produces error of less than  $\Delta E_{94} \leq 1.0$ .  $\Delta E_{94}$  and Spectral Reflectance RMS error were used to evaluate performance of predicting 800 random printed samples that each composed of only three colorants from C, M, Y, and K. 4 sets of primaries used by CNM and CKMM were  $2^3 = 8$  (0%, 100%),  $3^3 = 27$  (0%, 50%, 100%), and  $5^3 = 125$  (0%, 25%, 50%, 75%, 100%). The set of 8 primaries (0% and 100%) were used within the Neugebauer and Kubelka-Munk equations. For CNM, an increase from 8 primaries to 27 primaries considerably improved  $\Delta E_{94}$  and spectral reflectance RMS error. 125 primaries resulted in the target prediction accuracy ( $\Delta E_{94} \leq 1.0$ ). For CKMM, an increase from 8 primaries to 125 primaries could not achieve enough prediction accuracy.

### Four-Colorant Model Evaluation

Evaluation of  $\Delta E_{94}$  and Spectral Reflectance RMS error was used 800 random printed samples composed of four colorants in C, M, Y, and K. With consideration of the result of three-colorant evaluation, 3 sets of primaries as  $2^4 = 16$ ,  $3^4 = 81$ , and  $5^4 = 625$  used by CNM and CKMM. For CNM, more than 625 primaries were required to get the same prediction accuracy as the three-color evaluation. For CKMM, an increase from 16 primaries to 625 primaries could also not achieve enough prediction accuracy.

**Table 2. Three-Colorant Prediction Accuracy of CNM.**

The set of primaries	$2^3 = 8$	$3^3 = 27$	$5^3 = 125$
$\Delta E_{94}$ D65	6.26	1.53	1.13
Std.	2.77	0.78	0.61
Maximum	13.44	5.08	3.71
Minimum	0.48	0.09	0.11
$\Delta E_{94}$ ill A	6.94	1.64	1.13
RMS	0.036	0.011	0.006

**Table 3. Three-Colorant Prediction Accuracy of CKMM.**

The set of primaries	$2^3 = 8$	$3^3 = 27$	$5^3 = 125$
$\Delta E_{94}$ D65	7.78	4.72	2.89
Std.	4.30	2.74	1.54
Maximum	21.05	14.77	8.53
Minimum	0.69	0.33	0.14
$\Delta E_{94}$ ill A	8.72	5.33	3.20
RMS	0.031	0.027	0.018

**Table 4. Four-Colorant Prediction Accuracy of CNM.**

The set of primaries	$2^4 = 16$	$3^4 = 81$	$5^4 = 625$
$\Delta E_{94}$ D65	6.30	2.24	1.13
Std.	3.58	1.24	0.67
Maximum	16.06	6.87	3.43
Minimum	0.57	0.09	0.06
$\Delta E_{94}$ ill A	6.78	2.33	1.17
RMS	0.022	0.008	0.004

**Table 5. Four-Colorant Prediction Accuracy of CKMM.**

The set of primaries	$2^4 = 16$	$3^4 = 81$	$5^4 = 625$
$\Delta E_{94}$ D65	11.44	5.85	3.27
Std.	4.67	3.04	2.14
Maximum	26.24	16.83	9.60
Minimum	0.75	0.46	0.07
$\Delta E_{94}$ ill A	12.11	6.19	3.49
RMS	0.019	0.016	0.012

### Stability of Gray Balance

The stability of selective grays formed by sets of three dyes as C, M, and Y has been studied by a computer simulation method. A certain gray can be calculated by means of the Newton-Raphson technique on the assumption that Williams and Clapper formula<sup>18</sup> (7) holds for a color print, and that CNM (The set of primaries was  $5^3 = 125$ ) holds for a dye-based IJ.

$$R = 0.193T^{2.13} \left[ \frac{1}{2R_B} - \int_0^{\pi/2} T^{2\sec\theta} r_\theta \sin\theta \cos\theta d\theta \right]^{-1} \quad (7)$$

where

$T$  = transmittance of the gelatin layer

$R_B$  = reflectance of the baryta base is taken as 0.985

$\theta$  = angle of reflection of the light from the baryta base

$r_\theta$  = internal Fresnel reflectance of the interface  $\theta$

$R$  = reflectance when that of the baryta base is taken as 1.0

For the theoretical formula (7), surface reflection in a reflection-type color print was taken as 3 %. Peak density of C, M, and Y was taken as 4.0. The numerical integration was done with the Simpson's rule together with Newton's 3/8 rule<sup>19</sup> and all code was written in C.

Typical subtractive color dyes in a color print quoted from Ohta<sup>19</sup> were used in this study. Typical spectral density curves of C, M, and Y are shown in Fig. 2 after normalizing to 1.0 peak density. Spectral density curves of C, M, and Y that are used by a dye-based IJ are shown in Fig. 3.

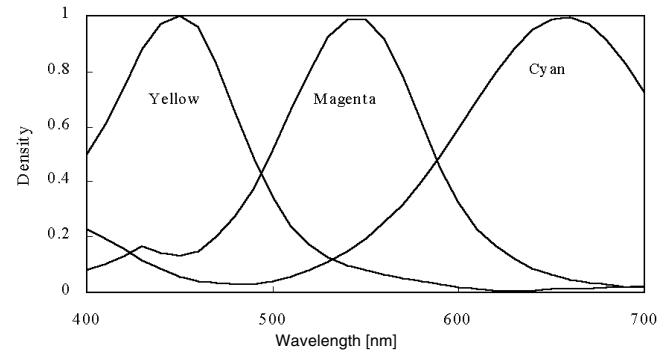


Figure 2. Spectral density of typical C, M, and Y dyes for a color print.

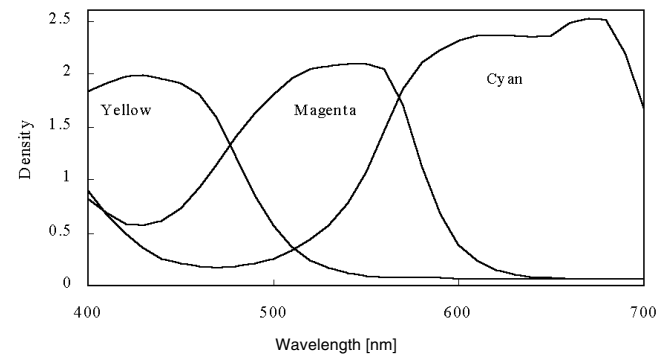


Figure 3. Spectral density of C, M, and Y dyes that is used by IJ.

Stability of gray balance was evaluated by metamerism index calculated as the CIE94 color difference under illuminant A for an estimated spectrum that resulted in a perfect colorimetric match under illuminant D65. Six lightness levels were probed where  $L^* = 30, 40, 50, 60, 70,$  and  $80$ . It can be seen in Fig. 4 that spectral density of selective grays in a dye-based IJ are wavier than those in a color print. The combination of three dyes in a color print gives a selective gray more stable by about 2.5 times that in a dye-based IJ as written in Table 6.

### Color Gamut Obtainable

The areas of color gamuts obtainable by C, M, and Y of Figs. 2 and Fig. 3 when they were used in a color print and in a

dye-based IJ were calculated at six lightness levels of  $L^* = 30, 40, 50, 60, 70,$  and  $80$ . It can be seen in Fig. 5 to Fig. 10 that the areas of color gamuts obtainable in a color print are smaller than those in a dye-based IJ. The former is larger by about 1.8 times than the latter in Table 7.

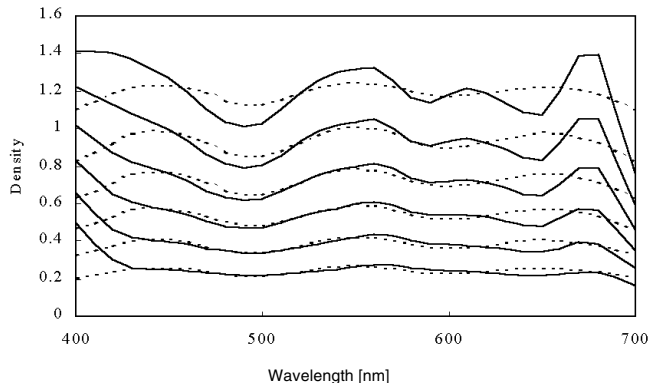


Figure 4. Spectral density of selective grays in a dye-based IJ (solid lines) and a color print (dotted lines).

Table 6. Index of Metamerism Illuminant A.

Lightness	Dye-based IJ	Color Print
$L^* = 80$	1.58	0.74
$L^* = 70$	2.17	0.99
$L^* = 60$	2.70	1.17
$L^* = 50$	3.10	1.29
$L^* = 40$	3.37	1.29
$L^* = 30$	3.16	0.79
Mean	2.68	1.05

Table 7. Comparison the Areas of Color Gamuts Obtainable in a Dye-Based IJ and a Color Print.

Lightness	Dye-based IJ	Color print
$L^* = 80$	4971	2983
$L^* = 70$	9002	5133
$L^* = 60$	12322	6538
$L^* = 50$	13616	6924
$L^* = 40$	11346	6039
$L^* = 30$	7113	3478
Mean	9728	5183

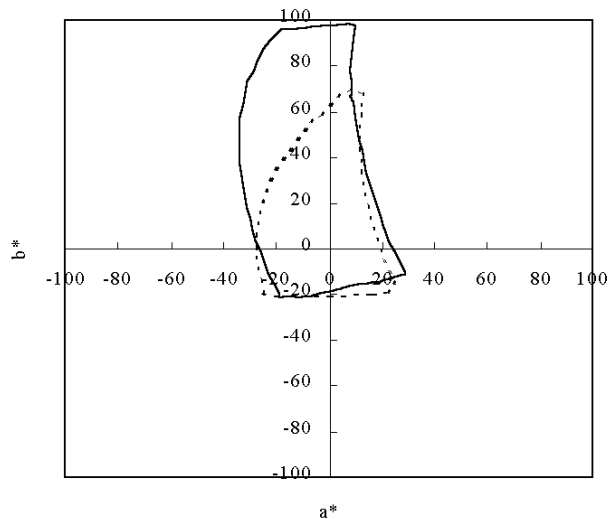


Figure 5. Color gamuts obtainable in a color print (dotted line) and a dye-based IJ (solid line) at  $L^* = 80$ .

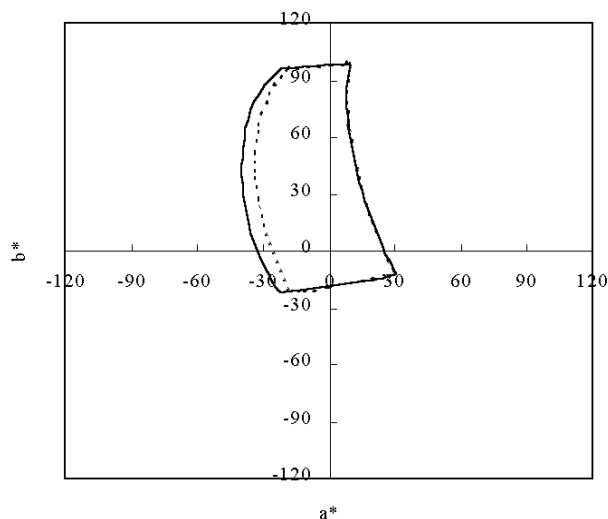


Figure 6. Color gamuts obtainable in a color print (dotted line) and a dye-based IJ (solid line) at  $L^* = 70$ .

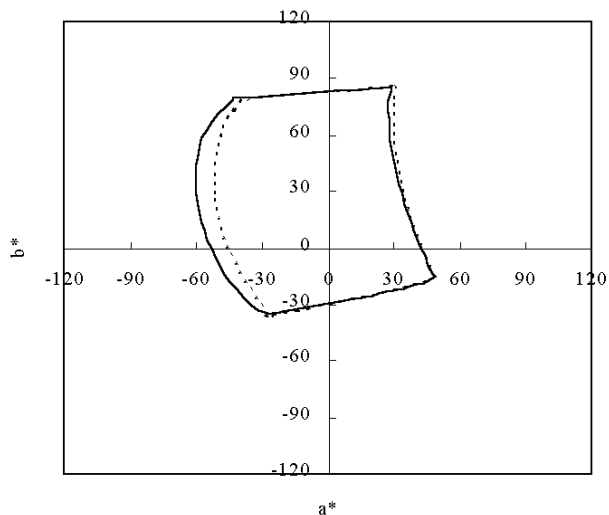


Figure 7. Color gamuts obtainable in a color print (dotted line) and a ye-based IJ (solid line) at  $L^* = 60$ .

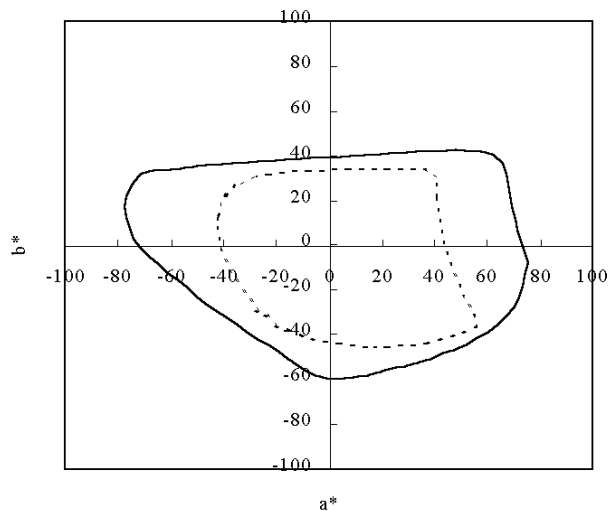


Figure 9. Color gamuts obtainable in a color print (dotted line) and a ye-based IJ (solid line) at  $L^* = 40$ .

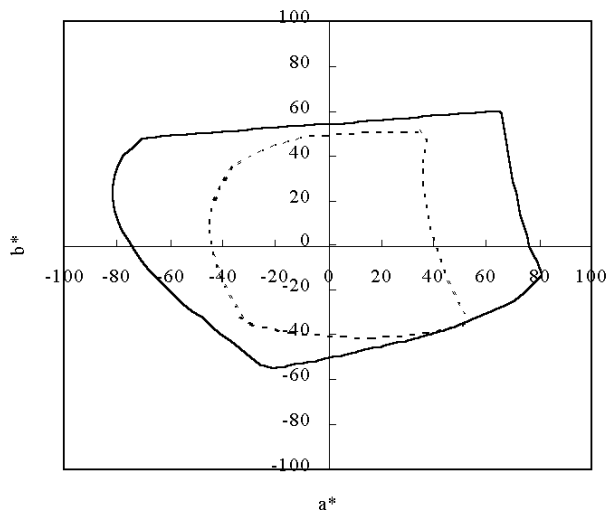


Figure 8. Color gamuts obtainable in a color print (dotted line) and a ye-based IJ (solid line) at  $L^* = 50$ .

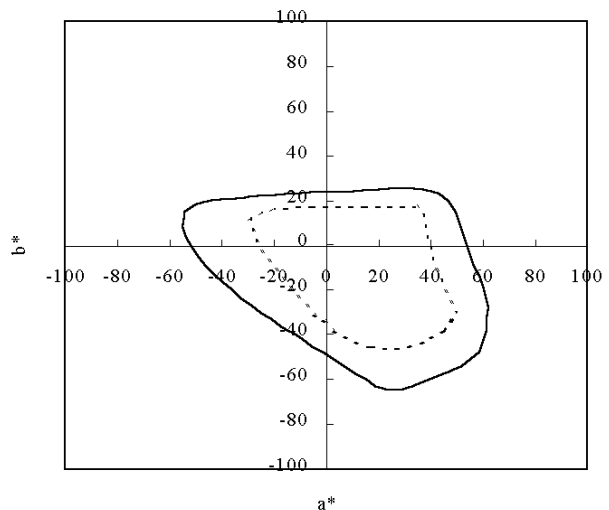


Figure 10. Color gamuts obtainable in a color print (dotted line) and a ye-based IJ (solid line) at  $L^* = 30$ .

### Conclusion

Five predicting models were compared by a dye-based IJ. Among these predicting models, only CNM resulted in  $\Delta E_{94} \cong 1.0$  when the set of primaries was  $5^{\text{colorants}}$  (the colorants power of 5). However this result is still inconvenient and unrealistic because it is necessary to print and measure a lot of points for prediction of reproduced tristimulus values. For example, 2-colorant prediction needs  $25 = 5^2$  primaries, 3-colorant prediction needs  $125 = 5^3$  primaries, 4-colorant prediction needs  $625 = 5^4$  primaries, 5-colorant prediction needs  $3,125 = 5^5$  primaries, and 6-colorant prediction needs  $15,625 = 5^6$  primaries.

Comparison of stability of gray balance and color gamut obtainable in color photography and IJ resulted in pointing out the problem that subtractive color dyes for IJs should be improved. The areas of color gamuts obtainable in a dye-based IJ were larger than those in a color print. However a selective gray in a color print was more stable than that in a dye-based IJ. Therefore, the optimum subtractive color dyes for IJs should be developed under consideration of gray balance.

### Acknowledgement

The authors would like to thank Mr. M. Rosen for his helpful suggestions.

## References

1. R. S. Berns, A. Bose, and D. Tzeng, "The Spectral Modeling of Large-Format Ink-Jet Printers", *RIT Munsell Color Science Laboratory Research and Development Final Report*, December 1996.
2. R. Balasubramanian, "Optimization of the spectral Neugebauer model for printer characterization", *Journal of Electronic Imaging*, **8(2)**, 156-166, (1999).
3. H. Kang, "Applications of Color Mixing Models to Electronic Printing", *J. Electr. Imaging*, **3**, 276-287, (1994).
4. L. A. Taplin and R. S. Berns, "Spectral Color Reproduction Based on a Six-Color Inkjet Output System", *IS&T/SID Ninth Color Imaging Conference*, (2001).
5. N. Ohta, "The Color Gamut Obtainable by the Combination of Subtractive Color Dyes", *Photogr. Sci. and Eng.*, **15(5)**, September-October, (1971).
6. N. Ohta, "The Color Gamut Obtainable by the Combination of Subtractive Color Dyes", *Photogr. Sci. and Eng.*, **16(3)**, May-June, (1972).
7. N. Ohta, "Stability of Selective Grey Obtainable by Use of Subtractive Colour Dyes", *Photogr. Sci. and Eng.*, **20**, (1972).
8. H. E. J. Neugebauer, "Die Theoretischen Grundlagen des Mehrfarbenedruckes", *Z. Wiss. Photog. Photophy. Photochem.*, **36**, 73-89, (1937).
9. J. A. C. Yule, *Principles of Color Reproduction*, John Wiley & Sons Inc., (1967).
10. B. Kruse and S. Gustavson, "Rendering of Color on Scattering Media", *Proc. SPIE*, **2657**, 422-431, (1996).
11. R. Balasubramanian, "Colorimetric Modeling of Binary Color Printers", *Proc. of IEEE International Conference on Image Processing*, Washington, DC, 2, 327-330, October 1995.
12. M. E. Demichel, *Proce'de'*, **26**, 17-21, 26-27, (1924).
13. J. A. C. Yule and W. J. Nielsen, "The Penetration of Light into Paper and Its Effect on Halftone Reproduction", *Proc. TAGA*, **4**, 66-75, (1951).
14. P. Kubelka, F. Munk, Ein Beitrag zur Optik der Farbanstriche, *Z. Tech Phys.* **12**, 593-601, (1931).
15. R. Rolleston and R. Balasubramanian, "Accuracy of Various Types of Neugebauer Models", *Proc. of the First IS&T/SID Color Imaging Conference*, Scottsdale, AZ, 32-37, November 1993.
16. A. U. Agar and J. P. Allebach, "An Iterative Cellular YNSN Method for Color Printer Characterization", *Proceedings of The Sixth IS&T/SID Color Imaging Conference*, 197-200, Scottsdale, AZ, November 17-20, (1998).
17. L. A. Taplin, "Spectral Modeling of a Six-Color Inkjet Printer", *M.S. Degree Thesis of Rochester Institute of Technology*, 3-8(2001).
18. F. C. Williams and F. R. Clapper, "Multiple Internal Reflections in Photographic Color Prints", *J.Opt. Soc. Amer.*, **43**, 595(1953).
19. N. Ohta, "Reflection Density of Multilayer Color Prints", *Photogr. Sci. and Eng.*, **15(6)**, November-December, (1971).

## Biographies

**Takayuki Ogasahara** received his BS and MS degrees in nuclear engineering from Nagoya University in 1994 and 1996. Since then, he has been employed at CANON INC. in Visual Information Technology Development Laboratory. His work has primarily focused on the development of image processing, including halftoning, borderless printing and image quality issues. He developed inkjet printers as S900 and S9000.

**Noboru Ohta** is the Xerox Professor in Color Engineering, Chester F. Carlson Center for Imaging Science, Rochester Institute of Technology. Between 1973 and 1976 he was a research associate at the National Research Council of Canada. He has authored over 80 technical publications in various aspects of color engineering and several textbooks including: "Color Engineering," and "The Fundamentals of Color Reproduction Engineering."